Chaos, Solitons & Fractals 45 (2012) 1328–1342

Contents lists available at SciVerse ScienceDirect

Chaos, Solitons & Fractals

Nonlinear Science, and Nonequilibrium and Complex Phenomena

journal homepage: www.elsevier.com/locate/chaos

Structurally unstable regular dynamics in 1D piecewise smooth maps, and circle maps ☆

Laura Gardini [a], Fabio Tramontana [b,*]

[a] Department of Economics, Society and Politics, Università degli Studi di Urbino, Via Saffi 42, 61029 Urbino, Italy
[b] Department of Economics and Business, Università degli Studi di Pavia, Via S. Felice 5, 27100 Pavia, Italy

ARTICLE INFO

Article history:
Received 24 March 2011
Accepted 10 July 2012

ABSTRACT

In this work we consider a simple system of piecewise linear discontinuous 1D map with two discontinuity points: $X' = aX$ if $|X| < z$, $X' = bX$ if $|X| > z$, where a and b can take any real value, and may have several applications. We show that its dynamic behaviors are those of a linear rotation: either periodic or quasiperiodic, and always structurally unstable. A generalization to piecewise monotone functions $X' = F(X)$ if $|X| < z$, $X' = G(X)$ if $|X| > z$ is also given, proving the conditions leading to a homeomorphism of the circle.

1. Introduction

The study of piecewise smooth systems is a quite recent field of research, because in several applied contexts, as in engineering, economics and social sciences, the models are ultimately described by piecewise smooth systems, either with continuous or discontinuous functions. These models are used, for example, for the transmission of chaotic signals, specially in telecommunication and engineering [7], or modelling systems with grazing bifurcations [30], and several other examples can be found in the survey books [8,14,42], as well as in economics (see [11,12,34,35]).

The peculiar feature of non smooth systems (continuous and discontinuous) is the occurrence of *border collision bifurcations*[1] (BCB henceforth), due to the collision of some invariant set (generally a periodic point) with the point in which the function changes its definition. This may lead to a drastic change, which may be impossible in the framework of smooth systems, for example the dynamics can change from an attracting fixed point suddenly to an attracting cycle of any period, or to chaotic dynamics, which is true (or strict) chaos, persistent as a function of the parameters (so called robust chaos in [6]).

Piecewise smooth systems may be classified in two classes having different properties, that is: *continuous* models and *discontinuous* models. The bifurcations occurring in piecewise smooth *continuous* unimodal maps can be investigated making use of the canonical form (a one-dimensional continuous unimodal piecewise-linear map) whose dynamics have been completely studied. The results are reported in [18,25,37] and other papers, [7,31,32,26,27], see also the recent survey in [36].

While regarding discontinuous one-dimensional piecewise-linear maps (frequently used in the applications, see [1–3,16]), only partial results exist. Several properties have been described, but still the knowledge is far from a complete classification of all the possible dynamics. The studies of discontinuous piecewise-linear maps started several years ago, and some works have been recently rediscovered. We recall, for example, the works by Leonov at the end of the 50th, [22,23] (and his results were used also in [25–29]). In his works Leonov described several bifurcations, giving a recurrence relation to find the analytic expression of the family of bifurcation curves occurring in a one-dimensional piecewise-linear map with one discontinuity point, which is still mainly unknown. His results have been recently improved in [15], dealing with the iterative process to detect analytically the equations of the BCB

☆ We thank two anonymous referees for their helpful comments that permitted us to improve the paper. This work has been performed within the activity of the project PRIN 2009 "Local interactions and global dynamics in economics and finance: models and tools", MIUR, Italy.

* Corresponding author.
E-mail addresses: laura.gardini@uniurb.it (L. Gardini), fabio.tramontana@unipv.it (F. Tramontana).

[1] The term is due to Nusse and Yorke in 1992 [31], see also [32].

0960-0779/$ - see front matter © 2012 Elsevier Ltd. All rights reserved.
http://dx.doi.org/10.1016/j.chaos.2012.07.007

curves, in the case of the so-called period adding scheme (or Farey scheme), and generalized in [4,41].

We recall that the generalization of this kind of dynamics to the case of increasing smooth functions with one discontinuity point, has been extensively investigated in the past, due to their connections with the flows, in particular with Lorenz like flows (but not only), and they are often called as *Lorenz maps* (see, for example, [20,10,24,33,5,21,9,17]).

Consider an invariant interval $I = [G(d),F(d)]$ with a discontinuity point $d \in I$ and $F(x)$ increasing in $[G(d),d]$ while $G(x)$ is increasing in $[d,F(d)]$. There is a drastic change in the dynamic behavior depending on the invertibility or non invertibility of the map in I. The bifurcation occurs when the following condition holds:

$$G \circ F(d) = F \circ G(d). \tag{1}$$

In such a case the map has the dynamics of a circle map, or homeomorphism of the circle (see [20,9,13]). When (1) holds, a rotation number can be identified for the circle map, which can be either rational or irrational. When a rational rotation number exists then all the trajectories have a cycle as ω-limit set. When the rotation number is irrational and the functions F and G are of class $\mathcal{C}^2$ then quasi periodic trajectories are dense in I, while if the functions F and G have not log (F') and log (G') with bounded variation, then the quasi periodic trajectories may be dense in a Cantor set attractor, or in I. When the rotation number is irrational the map is structurally unstable. When (1) holds and the functions are affine, then the circle map becomes a rotation, and either all the points are periodic of the same period (rational rotation number) or all the trajectories are quasiperiodic and dense in the interval I (irrational rotation number) (see also [15]).

When $G \circ F(d) < F \circ G(d)$ then the Lorenz map is into I, it is invertible, and it has a gap, or nonwandering interval, in I. Then no unstable cycle can exist (although the first derivative may be higher than 1in some interval) and the only possible dynamics are regular: the asymptotic state is ether a cycle, when the rotation number is rational, or a Cantor set when it is irrational. The case with irrational number is structurally unstable.

While when $G \circ F(d) > F \circ G(d)$ the Lorenz map is noninvertible in I and an invariant set with chaotic dynamics exists, even if the attracting set may be a cycle, a Cantor set[2] or chaotic intervals (see [20,9,19]).

To our knowledge, the bifurcation condition given in (1) has been found as a bifurcation condition in several applied models, leading from a regime of structurally stable regular dynamics to one of structurally stable chaotic behavior (as in [38,39]). However, a recent applied model, proposed in [40], is described by a peculiar map, very simple, whose dynamics are always in a state satisfying the condition given in (1). This family of maps is described by:

$$T:\ X' = \begin{cases} aX & \text{if } |X| < z \\ bX & \text{if } |X| > z \end{cases} \tag{2}$$

where the real parameters a and b can take positive or negative values, while $z > 0$. The parameter z is a scale variable, and by using the change of variable $x = X/z$, our model in (2) becomes the following map F:

$$F:\ x' = \begin{cases} f(x) = ax & \text{if } |x| < 1 \\ g(x) = bx & \text{if } |x| > 1 \end{cases} \tag{3}$$

which we rewrite as follows:

$$F:\ x' = \begin{cases} g(x) = bx & \text{if } x < -1 \\ f(x) = ax & \text{if } -1 < x < 1 \\ g(x) = bx & \text{if } x > 1 \end{cases} \tag{4}$$

So we have a one-dimensional piecewise linear discontinuous map, with two discontinuity points. As we shall see, in the parameter space satisfying $|a| > 1$ and $|b| < 1$ this family of maps is very special. The numerical simulations of the observed dynamics may lead to wrong conclusions, reflecting a sequence of states very close to a chaotic behavior. While no chaos can occur, any map of this family satisfies a stability condition equivalent to the one given in (1). Thus, this is a non-chaotic map with peculiar properties, with stable dynamics, periodic or quasiperiodic, but not attracting. That is, all the existing dynamic behaviors are structurally unstable in the sense that any perturbation in the parameters leads to a different dynamic behavior.

Clearly this peculiar condition can be broken by using piecewise smooth functions (instead of piecewise linear ones), examples of which will be given in the last section, or by changing the structure of the functions (for example assuming $f(x)$ or $g(x)$ affine instead of linear).

We remark that this model may be used to represent the interaction between two different dynamic behaviors in the same population, describing the interactions between two opposite tendencies, whichever is interpreted the population, in a social context, or in a financial market (as in [38] and [40]), or in some mechanical device.

The argument of the present paper belongs to those studied since the beginning of the theory of nonlinear dynamics, as originated from the Lorenz like systems or the Lorenz maps. Moreover, piecewise smooth systems are appearing since many years in all the applied disciplines. So, in our opinion, the results and open problems presented in this work are of interest in the study of complex phenomena in nonlinear sciences.

The rest of the paper is as follows. In Section 2 we summarize some generic properties of the map in (3), showing that the stability condition is always satisfied, whichever are the parameters a and b satisfying $|a| > 1$ and $|b| < 1$, in both the discontinuity points $x = -1$ and $x = 1$ (which are involved either separately or together). The peculiarity of the map is that we can analytically determine all the curves in the parameter space (a,b) which are associated with periodic orbits of any period. This is performed by using the Leonov's approach proposed in [15], starting with the computation of curves associated with the first complexity level, then using the adding mechanism to determine the analytic expressions of the curves associated with any complexity level, in an iterative way ([4]). The symmetry properties of this map are such that once that the curves in the region $a > 0$ and $b > 0$ (the so-called increasing/increasing case for $f(x)$ and $g(x)$) are obtained (in Section 3), all the other situations, associated with

[2] When a wondering interval exists.

increasing/decreasing, decreasing/increasing or decreasing/decreasing cases for the functions $f(x)$ and $g(x)$, are also immediately obtained, as shown in Sections 4 and 5. In Section 4 we prove that the increasing/decreasing case for $f(x)$ and $g(x)$ is reduced, by using the first return map, to a standard linear circle map (with increasing/increasing functions). In Section 5 we prove that the last two cases can be studied by using the second iterate of the map. Section 6 is devoted to a generalization of our class of maps to the piecewise smooth case. We first prove that when the stability conditions hold the system is reduced to a circle map, for which, in general, the case of rational rotation number is no longer structurally unstable as for the linear case. However, the stability condition can be considered not persistent, and breaking the stability condition the dynamics are lead to Lorenz maps, either to those characterized by noninvertibility (and with chaotic regimes) or to those characterized by invertibility (and thus to attracting cycles, now structurally stable). Two illustrative examples are given. Section 7 concludes.

2. The model and preliminary properties

In this section we are going to describe some simple properties of the map defined in (4). A first one is immediate from its structure. Performing the change of variable $y = -x$ the map is transformed into itself:

$$y' = \begin{cases} f(y) = ay & \text{if } |y| < 1 \\ g(y) = by & \text{if } |y| > 1 \end{cases} \tag{5}$$

which means that the phase space is symmetric with respect to the origin. We have so proved the following:

Property 1 (*Symmetry in the phase space*). *The map F in (3) is invariant with respect to the change of variable $y = -x$. Thus a periodic orbit $(x_1, x_2, \ldots, x_n)$ either has points symmetric with respect to the origin, or $(-x_1, -x_2, \ldots, -x_n)$ is also a periodic orbit.*

Even if, as we shall see, we can have cycles with periodic points in two or three partitions of the map, the functions involved are only two, so that the eigenvalue of a cycle only depends on the number of periodic points in which the functions $f(x)$ and $g(x)$ are applied. The following property immediately follows:

Property 2 (*Eigenvalue*). *The eigenvalue of a cycle of the map F in (3) having p periodic points in the middle region ($|x| < 1$) and q outside ($|x| > 1$) is given by $\lambda = a^p b^q$.*

Moreover, another property is also immediate, and excludes cases which are unfeasible in the applied context, as leading to divergent trajectories. From Property 2 we have that when both the slopes of the functions $f(x)$ and $g(x)$ are in modulus higher than 1, then all the possible cycles are unstable, as $|\lambda| > 1$. In these cases, a piecewise linear map, when bounded trajectories exist, can only have chaotic dynamics, or the trajectories are divergent. However, due to the particular structure of our map, when $|a| > 1$ and $|b| > 1$ we cannot have bounded dynamics because both the functions are linear. Thus, a trajectory in the range $|x| < 1$ is mapped in the region $|x| > 1$ in a finite number of iterations, and then the trajectory will be divergent. It follows that the unique possible existing cycle is an unstable fixed point. We have so proved the following:

Property 3 (*Divergence*). *Consider the map F with $|a| > 1$ and $|b| > 1$, then any initial condition $x \neq 0$ has a divergent trajectory.*

We can consider the regions in the parameter space (a,b), as summarized in Fig. 1 where the regions with divergent dynamics are those already introduced in Property 3, while those associated with the stability of the fixed point in the origin $O = (0,0)$ are described in the following.

Property 4 (*Fixed point*). *Consider the map F with $|a| < 1$ and $|b| < 1$, then the fixed point O in the origin is globally attracting.*

In fact, any initial condition in the range $|x| > 1$ has a trajectory which, in a few iterations, enters the range $|x| < 1$ from which the trajectory converges to the origin. This leads to the cental region in Fig. 1. While the dynamics in the other regions of the vertical strip in the center of Fig. 1 are described in the following.

Property 5 (*Fixed point and divergence*). *Consider the map F with $|a| < 1$ and $|b| > 1$, then the fixed point O is attracting, with basin of attraction $\mathcal{B}(O) =]-1, 1[$. Any i.c. x with $|x| > 1$ has a divergent trajectory.*

In fact, any initial condition in the range $|x| < 1$ has a trajectory which converges to the origin, as it is locally stable and the map is linear in that region, while any initial condition in the range $|x| > 1$, due to the structure of the piecewise linear map, has a trajectory which is divergent.

The particular cases with $a = 1$ and $a = -1$ are *degenerate bifurcations* (see [36]). For $a = 1$ there is the segment $]-1,1[$ filled with fixed points, while for $a = -1$ the segment $]-1,1[$ is filled with cycles of period 2. At these degenerate bifurcations the existing cycles are stable but not asymptotically stable (i.e., not attracting the trajectories of nearby points).

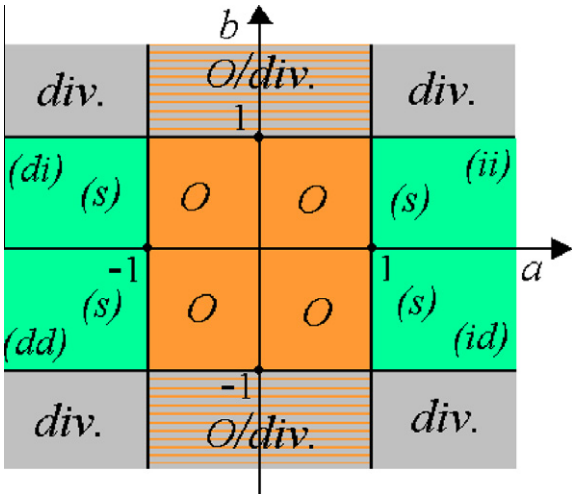

Fig. 1. Two dimensional parameter space (a,b). The regions are bounded by the straight lines $a = \pm 1$ and $b = \pm 1$.

After the bifurcation, for $|a| > 1$, the result depends on the modulus of b. As we have seen, for $|b| > 1$ only divergent dynamics can occur, while for $|b| < 1$ an invariant absorbing interval J exists, given by:

$$J = [f(-1), f(1)] = [-a, a], \quad \text{if } a > 1 \qquad (6)$$
$$J = [f(1), f(-1)] = [a, -a], \quad \text{if } a < -1$$

attracting the trajectories of all the points of the phase space outside J (and from which a trajectory cannot escape), thus the dynamics cannot be divergent.

It follows that the particular cases left to our analysis are exactly those in the green regions of Fig. 1, which is the main object of our work. As remarked in Fig. 1 the regions which are to be investigated are really four different ones, associated with different values of the slopes of the functions $f(x)$ and $g(x)$. For $a > 0$ these include the two cases

$$F(ii),\ \text{increasing/increasing}: \quad a > 1,\ 0 < b < 1 \qquad (7)$$
$$F(id),\ \text{increasing/decreasing}: \quad a > 1,\ -1 < b < 0$$

while for $a < 0$ these include the two cases

$$F(di),\ \text{decreasing/increasing}: \ a < -1,\ 0 < b < 1 \qquad (8)$$
$$F(dd),\ \text{decreasing/decreasing}: \ a < -1,\ -1 < b < 0$$

In the next sections we shall completely explain the cases $F(ii)$ and $F(id)$ and these will also be used to explain the cases $F(di)$ and $F(dd)$. Let us first introduce in this section what is the peculiar property of the map F, which is stated in the following:

Stability property. *Consider the map F with $|a| > 1$ and $|b| < 1$, then the following equalities hold*:

$$(S1): \quad f \circ g(1) = g \circ f(1) \qquad (9)$$
$$(S2): \quad f \circ g(-1) = g \circ f(-1) \qquad (10)$$

In fact, both properties can be immediately verified from the definition of the map F given in (3): we have $g \circ f(1) = ba$ and $f \circ g(1) = ab$ as well as $g \circ f(-1) = -ba$ and $f \circ g(-1) = -ab$, so that the properties in (9) and (10) hold. □

As already remarked in the Introduction, the Stability Property is important because it leads to a *stability regime* which is however structurally unstable. The important dynamic property of the map F is exactly this Stability Property which, as we shall see, *implies that an invariant set A exists, and each point of A has a unique rank-1 preimage in the set A itself*. As we shall see, this leads to the same property of a linear rotation on a circle, and depending on a suitable rotation number, which in our case is associated with the values of the parameters a and b, a trajectory may be either periodic (in which case all the points in A are periodic of the same period), or quasiperiodic and dense in A. In the case increasing/increasing $F(ii)$, considered in the next section, there are two disjoint invariant absorbing intervals: $A = I^L \cup I^R \subset J$; while in the case increasing/decreasing $F(id)$, that we shall consider after, the invariant set A is the union of two different intervals (not invariant).

Let us first analyze the conditions leading to periodic dynamics. Let x be a point belonging to the invariant absorbing set A of the map F, different from a discontinuity point, then it can be a periodic point of first period n if n is the smallest integer such that $F^n(x) = x$. Then let p be the number of periodic points of the n-cycle in the region $|x| < 1$ and q in the region $|x| > 1$, $(p + q) = n$. Then we have

$$F^n(x) = a^p b^q x. \qquad (11)$$

It follows that the condition of periodic orbit, $a^p b^q x = x$, can be satisfied by a point $x \neq 0$ iff the eigenvalue $\lambda = a^p b^q$ of the cycle satisfies the following equation

$$a^p b^q = 1 \qquad (12)$$

We have so proved the following

Property 6 (*Cycles*). *Consider the map F with $|a| > 1$ and $|b| < 1$, then x is a periodic point of an n-cycle iff $a^p b^q = 1$ holds, where p is the number of periodic points of the n-cycle in the region $|x| < 1$ and q in the region $|x| > 1$, with $(p + q) = n$ and the eigenvalue of the cycle is $\lambda = a^p b^q = 1$.*

On the other hand, the fact that the eigenvalue is equal to 1, in the piecewise linear case means that the cycle is stable but not attracting, and this can only occur for all the points of an interval. That is, the map F necessarily satisfies the condition $F^n(x) = x$ for all the points x of a suitable interval or intervals, invariant for F^n, all the points of which are periodic of the same period and with the same symbolic sequence (i.e., with the same sequence of applied functions $f(x)$ and $g(x)$, cyclically invariant). Examples shall be given in the next sections, where the different cases are considered.

3. Dynamics in the increasing/increasing case $F(ii)$

Let us consider here the effects of the properties $(S1)$ and $(S2)$ in (9) and (10) on the dynamics, when the map has the two functions $f(x)$ and $g(x)$ both with positive slopes, $a > 1$ and $0 < b < 1$ as qualitatively shown in Fig. 2a.

Under such assumptions the map leads to two coexisting invariant absorbing intervals, and thus *we necessarily have bistability*. In fact, any initial condition in the region $x > 0$ will be forever in that region, entering the absorbing interval $I^R = [g(1), f(1)]$ in a finite number of iterations, from which it cannot escape. Thus it attracts the points in $\mathcal{B}(I^R) =]0, +\infty[$, which is its basin of attraction. The restriction of the map F to the absorbing interval I^R is given by

$$F^R: \quad x' = \begin{cases} f(x) = ax & \text{if } g(1) < x < 1 \\ g(x) = bx & \text{if } 1 < x < f(1) \end{cases} \qquad (13)$$

where $g(1) = b \in (0,1)$ and $f(1) = a > 1$.

From Property 1 we can deduce that any initial condition in the region $x < 0$ will be forever in that region, entering the absorbing interval $I^L = [f(-1), g(-1)]$ in a finite number of iterations, from which it cannot escape, and it attracts the points in $\mathcal{B}(I^L) =]-\infty, 0[$. The restriction of the map F to the absorbing interval I^L is given by

$$F^L: \quad x' = \begin{cases} g(x) = bx & \text{if } f(-1) < x < -1 \\ f(x) = ax & \text{if } -1 < x < g(-1) \end{cases} \qquad (14)$$

where $f(-1) = -a < -1$ and $g(-1) = -b \in (-1,0)$. So we are lead to the invariant set

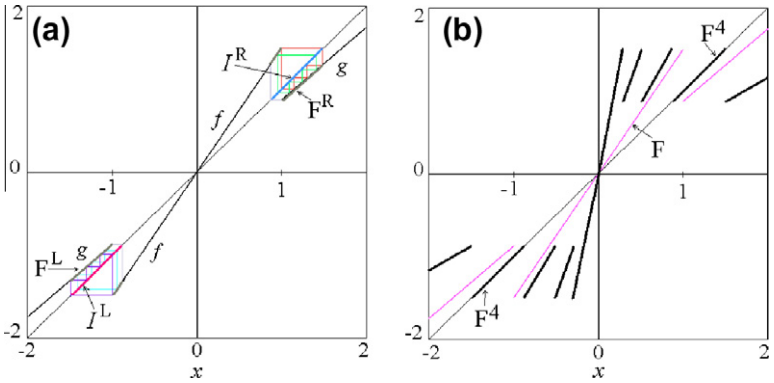

Fig. 2. In (a) Map F in the case $F(ii)$ at $a = 1.5$ and $b = 0.87358$.

$$A = I^L \cup I^R = [f(-1), g(-1)] \cup [g(1), f(1)]. \tag{15}$$

As no divergent trajectory can occur, we can argue that an initial condition in one of the intervals converges to some attracting set. However this is not the case. An attracting set (or attractor) is defined as some invariant set for which a neighborhood exists whose points converge to the attractor. But this cannot occur in our map. In fact, it is known (see e.g., [20,9], to cite a few), that in the case of an increasing discontinuous map the stability property leads to a circle map (we shall return on this in Section 6), but in the particular case of linear functions (as we have) the map is conjugate with a linear rotation (see also [13] and [15]). This means that depending on the values of a and b a suitable rotation number may be defined, which may be rational or irrational, and cannot be persistent. For a rational rotation number all the points of the absorbing intervals $I^{R/L}$ are periodic (and all of the same period), for an irrational rotation number all the points of the absorbing intervals $I^{R/L}$ have quasiperiodic trajectories dense in the absorbing intervals $I^{R/L}$, but not chaotic. Thus in the rational case no true attracting set can exist, but the dynamics are regular: when there are periodic orbits these are stable but not attracting. Similarly when there are quasiperiodic trajectories. And in the case of a linear rotation (differently from a generic circle map), these dynamics are structurally unstable, as the rational or irrational rotation number cannot be persist as the parameters are varied.

An example of periodic orbits is shown in Fig. 2 for the case $F(ii)$ at $a = 1.5$ and $b = 0.87358$ (the reason why of this value is explained below), and at these values of the parameters we have that all the points of the invariant intervals I^R and I^L are periodic of period 4 (see Fig. 2a). The fourth iterate of the map is shown in Fig. 2b and it consists in several branches, one of which belongs to the diagonal on the invariant interval I^R, and a second branch on the diagonal, on the interval I^L.

The main result for our map is that *this dynamic property is always true, independently on the values of the slopes*, in the regions marked with (S) in Fig. 1. That is, for the map F we are interested in, this kind of non-chaotic regime, characterized by structurally unstable orbits (either periodic or quasiperiodic), is persistent for all the parameters in the cases $F(ii)$, $F(id)$, $F(di)$ and $F(dd)$ here defined.

Let us consider a few more properties on the organization of the existing cycles. We have seen Property 6 in the previous section, which states when a cycle can exist. So we can find the exact values of p and q giving us the cycles, and it is possible to organize in some way their existence regions (which are curves in the two-dimensional parameter plane (a,b)).

In the case $F(ii)$, we can follow the same technique used in the case of attracting cycles when the *period adding scheme works*. Indeed, as shown in [15], the intersection of the existing periodicity regions with the locus $(S1)$ of the stable (but not attracting) regime where Property $(S1)$ holds, is a set of points in the locus which still follows the adding mechanism. So we can reason similarly in our case. It is clear that in order to have the sequence of a so-called maximal cycle in the interval I^R, say with symbolic sequence fg^k, we have to look for a periodic point which can be obtained as a fixed point of the composite function $g^k \circ f(x)$, by solving the equation $g^k \circ f(x) = x$. For their existence we have to determine all the parameters a and b that, for any $k \geqslant 1$, satisfy

$$fg^k: \quad ab^k = 1. \tag{16}$$

Thus we have curves in the parameter plane (a,b) a few of which (for $k = 1,\ldots,10$) are drawn in Fig. 3a. For $k = 3$ we have the 4-cycles, so that for $a = 1.5$ we have computed from (16) the value $b = 0.87358$, used to show the example in Fig. 2.

Following the adding mechanism, between any two consecutive curves associated with maximal cycles, or cycles of first level of complexity, we can find two families of infinite curves associated with cycles of second level of complexity. For example, between the two curves fg^k and fg^{k+1} we have the following pair of families of infinite curves (both for any $m \geqslant 1$):

$$(fg^k)^m fg^{k+1}: \quad a^{1+m}b^{k+1+mk} = 1 \tag{17}$$

$$fg^k(fg^{k+1})^m: \quad a^{1+m}b^{k+m(1+k)} = 1. \tag{18}$$

A few of these curves in the region (ii) are shown in Fig. 3b for $k = 1,\ldots,10$ and $m = 1,2,3$.

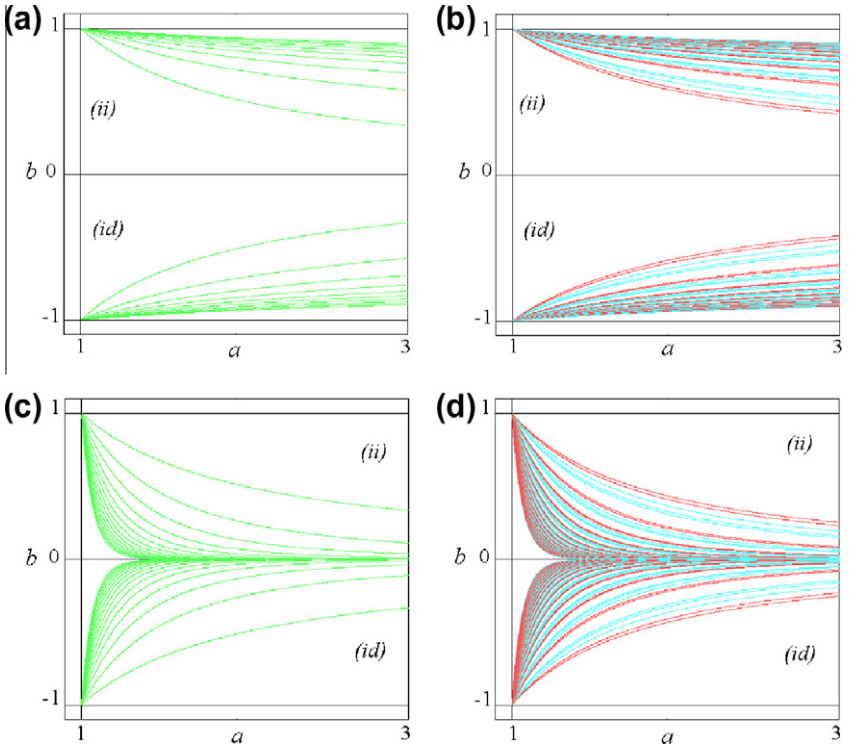

Fig. 3. In (a), in the parameter plane (a,b) region (ii), curves associated with periodic orbits, whose equation is given in (16), for $k = 1,\ldots,10$. In the region (id) the symmetric ones. In (b) curves associated with periodic orbits, whose equation is given in (17) and (18) for $k = 1,\ldots,10$ and $m = 1,2,3$. In (c), in the region (ii), curves associated with periodic orbits, whose equation is given in (19), for $k = 1,\ldots,10$, and in the region (id) the symmetric ones. In (d) curves associated with periodic orbits, whose equation is given in (20) and (21) for $k = 1,\ldots,10$ and $m = 1,2,3$, belonging to the region (ii), and in the region (id) the symmetric ones are drawn.

Similarly we can continue for any level of complexity: between any two consecutive curves, with symbolic sequence A and B, of the same level of complexity, we can compute two families of infinitely many curves, with symbolic sequence $(A)^nB$ and $A(B)^n$, for any $n \geqslant 1$.

Exchanging f and g we obtain a maximal cycle existing in the interval I^R, with different symbolic sequence: gf^k. A periodic point can be obtained as a fixed point of the function $f^k \circ g(x)$, so we have to determine all the parameters a and b such that, for any $k \geqslant 1$:

$$gf^k: \quad ba^k = 1 \tag{19}$$

and two families of curves of cycles of second complexity level are given, for any $m \geqslant 1$, by:

$$(gf^k)^m gf^{k+1}: \quad b^{1+m}a^{k+1+mk} = 1 \tag{20}$$

$$gf^k(gf^{k+1})^m: \quad b^{1+m}a^{k+m(1+k)} = 1 \tag{21}$$

and so on for any level of complexity. A few of the curves in (19) are illustrated in the region (ii) in Fig. 3c for $k = 1,\ldots,15$. In Fig. 3d the curves from Eqs. (20) and (21) are shown for $k = 1,\ldots,15$ and $m = 1,2,3$. We recall that when the parameters belong to such curves, there are cycles in the invariant interval I^R and the symmetric ones also exist in the other invariant interval I^L. Under assumption $F(ii)$, the infinitely many curves for which the parameters (a,b) are associated with periodic orbits, are dense in the region defined as (ii). However, if we numerically compute a bifurcation diagram, we observe a figure as the one shown in Fig. 4, where the variable x is reported as a function of b at $a = 1.5$ fixed.

The region corresponding to assumption $F(ii)$ is the interval $0 < b < 1$, and we have two disjoint and coexisting

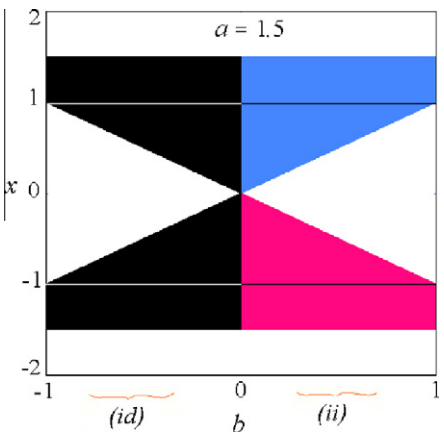

Fig. 4. One dimensional bifurcation diagram of the map F showing the variable x is as a function of b at $a = 1.5$ fixed. The case $F(ii)$ occurs for $b > 0$: dynamics in two disjoint attracting intervals. The case $F(id)$ occurs for $b < 0$: dynamics in a unique attracting set.

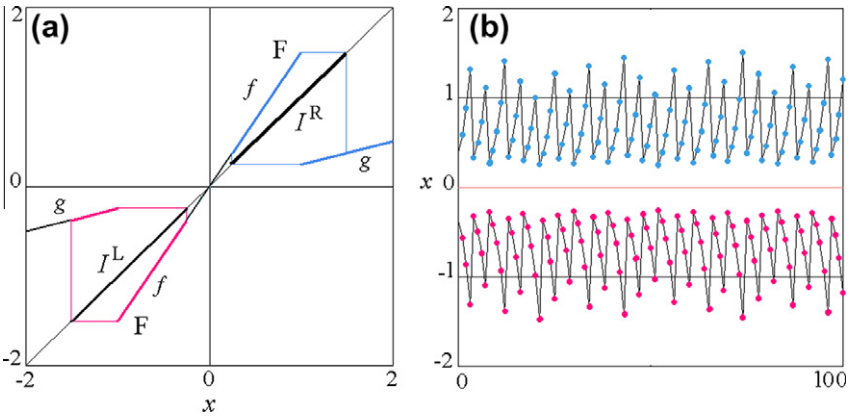

Fig. 5. In (a) Map F in the case $F(ii)$ at $a = 1.5$ and $b = 0.25$. In (b) versus time behavior of two coexisting trajectories at the same parameter values as in (a).

invariant absorbing intervals I^R (in blue/light grey in Fig. 4) and I^L (in red/dark grey in Fig. 4). The numerical results are qualitatively similar to those which can be obtained in a chaotic regime. However, no chaotic regime can here exist. As at all the parameter values either there are periodic points or quasiperiodic trajectories, and due to the fact that both the values of periodic orbits and quasiperiodic orbits are dense in the interval, we can numerically observe mainly a quasiperiodic orbit.

We notice that also the versus time trajectory may be misleading. It may be considered as chaotic while it cannot be. An example is shown in Fig. 5. In Fig. 5b the versus time behaviors of two coexisting trajectories are shown, one in the absorbing interval I^R and the other in the absorbing interval I^L.

4. Dynamics in the increasing/decreasing case $F(id)$

Let us here consider the parameters which satisfy conditions $F(id)$. Even if the function f is increasing and g decreasing in their definition sets, see an example in Fig. 6a, the existence of the properties in (9) and (10) implies that *the map F* in (3) is uniquely invertible in the invariant absorbing set *A given by*

$$A = [f(-1), g(1)] \cup [g(-1), f(1)]. \tag{22}$$

In fact, consider the interval $[f(-1),g(1)] = [f(-1),f(g(1))] \cup [g(f(1)),g(1)]$ (where we have used $f(g(1)) = g(f(1))$), then each point of $[f(-1),f(g(1))]$ has only the inverse via f^{-1} in A, while each point of $[g(f(1)),g(1)]$ has only the inverse via g^{-1} in A (as in both cases the other one is external to A). Similarly in the other interval $[g(-1),f(1)] = [g(-1),\ g(f(-1)] \cup [f(g(-1)),f(1)]$ (where we have used $g(f(-1)) = f(g(-1))$), each point of $[g(-1),g(f(-1)]$ has only the inverse via g^{-1} in A while each point of $[f(g(-1)),f(1)]$ has only the inverse via f^{-1} in A (as in both cases the other one is external to A).

This means that F is invariant in A and each point of A has one and only one preimage, which is characteristic of a circle map. The properties of F can be studied by using the first return map, say map F_r, in a suitable interval. As a trajectory from the side $x < 0$ can "return" to the right side $x > 0$ *only* via an application of the function $g(x)$ when $x < -1$, we can consider the first return in the first interval on the right side, that is in $r = [g(-1),g(f(-1))] = [-b, -ab]$, and we can prove the following proposition:

Proposition 1. *The first return map F_r of F in the case (id) $(a > 1, -1 < b < 0)$ in the interval $r = [-b, -ab]$, is a piecewise linear map made up of increasing branches, with a unique discontinuity point in the preimage of -1 belonging to r, and conjugated with a linear rotation.*

Proof. Let us define as $\xi$the first preimage of the point $x = -1$ in r. That is, for a suitable $k > 0$, we have

$$\xi = -\frac{1}{ba^k} \in r \tag{23}$$

so that the first return map is defined as

$$F_r: \quad x' = \begin{cases} T_l(x) = b^2a^{k+1}x & \text{if } -b \leqslant x < \xi \\ T_r(x) = b^2a^k x & \text{if } \xi < x \leqslant -ab \end{cases} \tag{24}$$

and it is immediate to verify that $T_l(\xi) = -ab, T_r(\xi) = -b$, and $T_r \circ T_l(\xi) = -b^3a^{k+1} = T_l \circ T_r(\xi)$, so that F_r is a linear circle map in r, conjugated with a rotation. □

An example in shown in Fig. 6a, where $k = 6$, and the first return map is enlarged in Fig. 6b. It follows that in the set A the map has either all periodic points dense in A or quasiperiodic trajectories dense in A. A numerically obtained bifurcation diagram is shown in Fig. 4 at $a = 1.5$ fixed, in the region corresponding to assumption $F(id)$ which is the interval $-1 < b < 0$. Although the figure suggests a chaotic behavior, it is not. The dynamics in the case $F(id)$ are similar to those described in the case (ii), and we can analytically write the curves in the parameter plane at which we can find all periodic orbits of any level of complexity. In Fig. 3 we can see the curves described in the previous section *reflected in the region* (id). These curves correspond to parameters associated with a rational rotation and cycles of suitable periods exist for the map F in the case (id), as stated in the following proposition:

Proposition 2. *Let $(\bar{a}, \bar{b})$ be a point of the parameter plane belonging to a curve in the region (ii) associated with n-cycles of F, then also the point $(\bar{a}, -\bar{b})$ in the region (id) belongs to a curve associated with periodic orbits of F, of period n or 2n.*

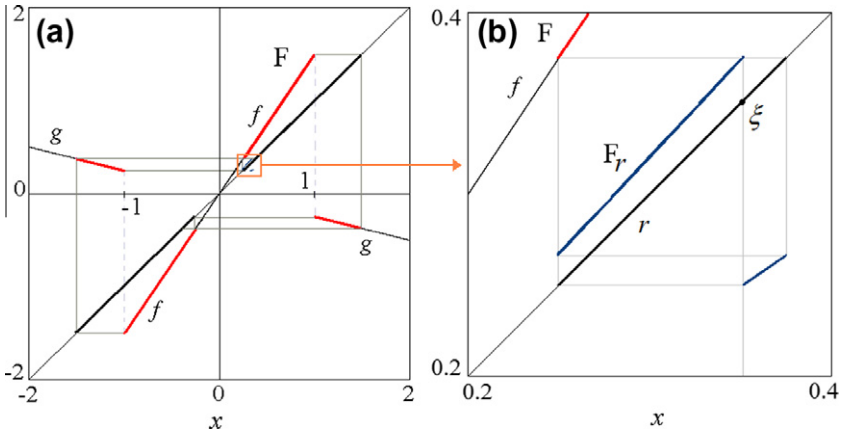

Fig. 6. (a) Map F in the case $F(id)$ at $a = 1.5$ and $b = -0.25$. In (b) enlargement showing the first return map F_r in the interval $r = [g(-1), g(f(-1))]$.

Proof. Let us assume that for $(\bar{a}, \bar{b}) \in (ii)$ the condition

$$\bar{a}^p \bar{b}^q = 1 \tag{25}$$

occurs for some suitable integers p and q with $n = p + q$. Then *if q is even we also have*

$$\bar{a}^p (-\bar{b})^q = 1 \tag{26}$$

in which case the symmetric curve is associated with *a cycle of the same period* $(n = p + q)$. Otherwise, *if q is odd we have* $\bar{a}^p (-\bar{b})^q = -1$ *and*

$$\bar{a}^{2p} (-\bar{b})^{2q} = 1 \tag{27}$$

which means that the symmetric curve corresponds to *a cycle of double period* $(2n = 2(p + q))$. □

For example, at $(a,b) = (1.5, 0.903602)$, belonging to a curve in the region (ii) (from (16) with $k = 4$) associated with a 5-cycle having $p = 1$ and $q = 4$, at $(a, -b) = (1.5, -0.903602)$ (see Fig. 7a) we must have 5-cycles, as shown in Fig. 7b.

In the case of the 4-cycle shown in Fig. 2 at $(a,b) = (1.5, 0.87358)$ we have $p = 1$ and $q = 3$, thus at $(a, -b) = (1.5, -0.0.87358)$ we must have 8-cycles, as shown in Fig. 8.

5. Dynamics in the cases *F(di)* and *F(dd)*

The dynamics in these cases are similar to those described in the previous two Sections. In some situations (when $|ab| < 1$) they can be reduced to the cases $F(ii)$ and $F(id)$ by using the second iterate of the map, as stated in the following Proposition.

Proposition 3. *Consider map F when $a < -1$ and $|ab| < 1$, then the second iterate F^2 is continuous in the points $x = 1$ and $x = -1$, discontinuous in the points $x_l = \frac{1}{a}$ and $x_r = -\frac{1}{a}$. The case F(di) is conjugated with the case F(id) while the case F(dd) is conjugated with the case F(ii).*

Proof. Let $a < -1$, then the rank-1 preimages of the discontinuity points $x = 1$ and $x = -1$ of the function f exist inside the range $|x| < 1$. Explicitly, the preimages are given by

$$-1 < x_l = \frac{1}{a} < 0, \quad 0 < x_r = \frac{-1}{a} < 1 \tag{28}$$

satisfying $f(x_l) = 1$ and $f(x_r) = -1$. Clearly these two points are discontinuity points for the second iterate F^2 of the map. While the continuity of the map F^2 in the points $x = 1$ and $x = -1$ is an immediate consequence of the

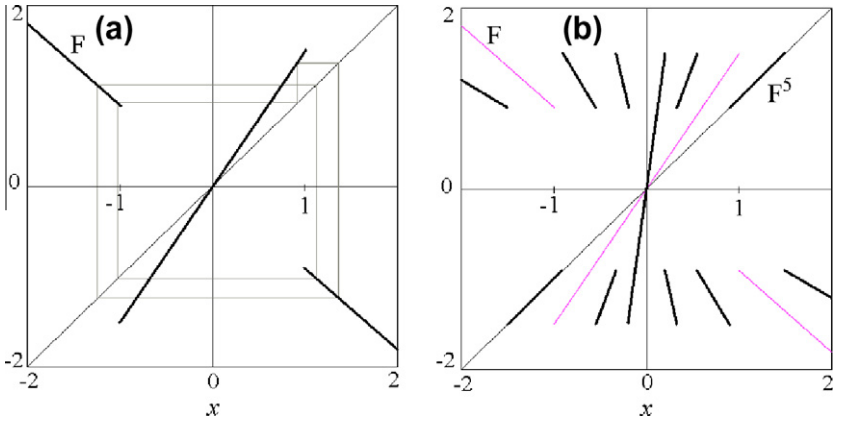

Fig. 7. In (a) Map F at $(a, -b) = (1.5, -0.903602)$. In (b) Map F and map F^5 at the same parameter values.

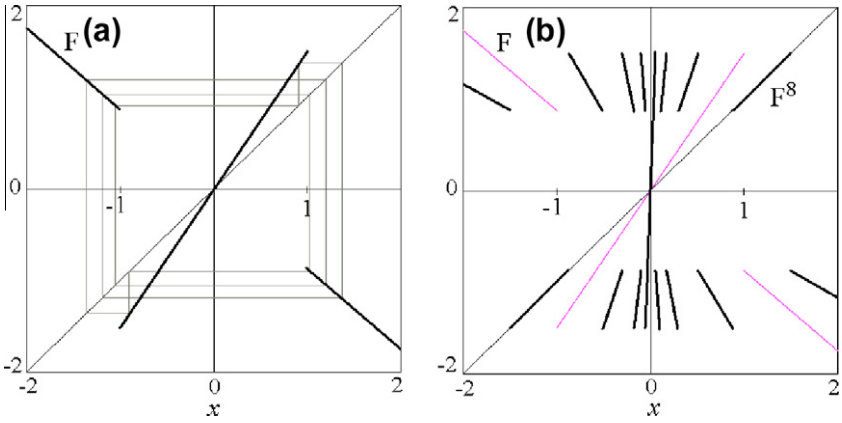

Fig. 8. In (a) Map F at $(a, -b) = (1.5, -0.0.87358)$. In (b) Map F and map F^8 at the same parameter values.

Stability Property: from $f \circ g(1) = g \circ f(1)$ we have $lim_{x\to 1-}F^2(x) = lim_{x\to 1+}F^2(x)$ while from $f \circ g(-1) = g \circ f(-1)$ we have $lim_{x\to(-1)-}F^2(x) = lim_{x\to(-1)+}F^2(x)$. The map F^2 is defined by a linear increasing function (i.e., with positive slope):

$$f^2(x) = a^2 x \tag{29}$$

in the interval $x_l < x < x_r$, while outside it is given by

$$f \circ g(x) = g \circ f(x) = abx \tag{30}$$

and it is increasing or decreasing depending on the sign of the parameter b. Thus:

- In the case $F(di)$, with $b > 0$, outside the interval (x_l, x_r) the second iterate F^2 is a negative sloped function, so that F^2 is topologically conjugated with the increasing/decreasing case already considered in (id), with discontinuity points in x_l and x_r in place of -1 and 1, respectively, and slopes given by $a^2 > 0$ and $ab < 0$ in place of a and b, respectively;
- In the case $F(dd)$, with $b < 0$, outside the interval (x_l, x_r) the second iterate F^2 is a positive sloped function, so that F^2 is topologically conjugated with the increasing/increasing case already considered in (ii), with discontinuity points in x_l and x_r in place of -1 and 1, respectively, and slopes given by $a^2 > 0$ and $ab > 0$ in place of a and b, respectively. □

An example in the case $F(di)$ (resp. $F(dd)$) is shown in Fig. 9a (resp. Fig. 9b). When $|ab| > 1$ the discontinuity points of F have more than two preimages in the absorbing interval, so that the second iterate F^2 has more than two discontinuities and the similarity with the previous cases is no longer immediate. However, that the results hold comes from the existence of dense curves in the parameter space. In fact, regarding the curves associated with rational rotation numbers, we can take advantage of those existing in the regions (ii) with $a > 1$, as stated in the following proposition:

Proposition 4. *Let $(\bar{a}, \bar{b})$ be a point of the parameter plane belonging to a curve in the region (ii) associated with n- cycles of F, then also the point $(-\bar{a}, \bar{b})$ in the region (di) and the point $(-\bar{a}, -\bar{b})$ in the region (dd) belong to curves associated with periodic orbits of F, of period n or 2n.*

Proof. Let us consider the parameters $(\bar{a}, \bar{b})$ belonging to a curve in the region (ii) $(a > 1, 0 < b < 1)$ assuming $n = p + q$ such that

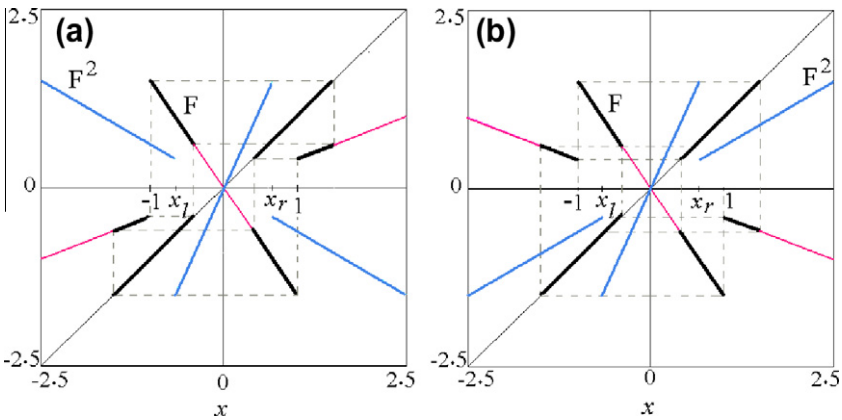

Fig. 9. In (a) Map F in the case $F(di)$ at $a = -1.5$ and $b = 0.4$. In (b) Map F in the case $F(dd)$ at $a = -1.5$ and $b = -0.4$.

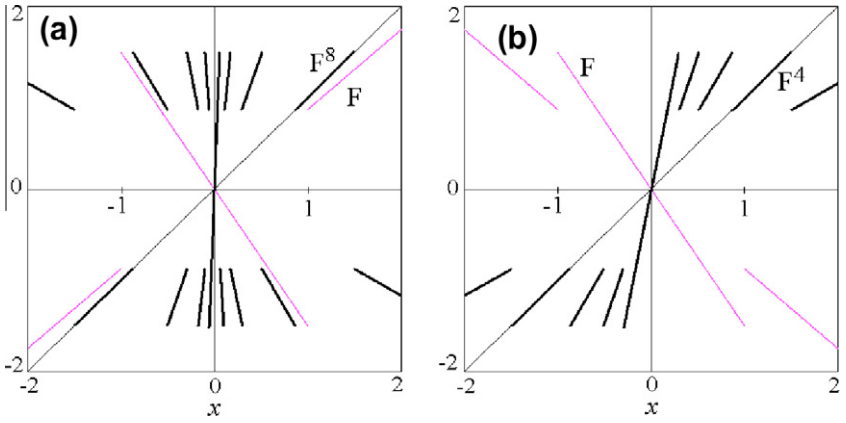

Fig. 10. In (a) Map F and map F^8 at $(-a,b) = (-1.5,0.87358)$, in the case $F(di)$. In (b) Map F and map F^4 at $(-a,-b) = (-1.5,-0.87358)$, in the case $F(dd)$.

$$\bar{a}^p \bar{b}^q = 1. \tag{31}$$

Then, if p *is* even we also have

$$(-\bar{a})^p \bar{b}^q = 1 \tag{32}$$

in which case the symmetric curve in the region (di) is associated with *a cycle of the same period* $(n = p + q)$. Otherwise, if p is odd we have $(-\bar{a})^p \bar{b}^q = -1$ and

$$(-\bar{a})^{2p} \bar{b}^{2q} = 1 \tag{33}$$

which means that the symmetric curve in the region (di) corresponds to *a cycle of double period* $(2n = 2(p + q))$.

While considering the symmetric point $(-\bar{a}, -\bar{b})$ in the region (dd), we necessarily have

$$(-\bar{a})^p (-\bar{b})^q = 1 \tag{34}$$

when p and q are *both even or both odd*, in which case we have *cycles of the same period*, while when p and q are *one odd and one even*, from $(-\bar{a})^p (-\bar{b})^q = -1$ we have

$$(-\bar{a})^{2p} (-\bar{b})^{2q} = 1 \tag{35}$$

which leads to *cycles of double period*. □

An example is shown in Fig. 10. Considering the case in Fig. 2, at $(a,b) = (1.5,0.87358)$, belonging to a curve in the region (ii) associated with 4-cycles with $p = 1$ and $q = 3$, at $(-a,b) = (-1.5,0.87358)$ we must have 8-cycles, as it is shown in Fig. 10a, while at $(-a,-b) = (-1.5,-0.87358)$ we must have 4-cycles, as shown in Fig. 10b.

From the Properties 2 and 4 it is clear that the curves associated with periodic orbits existing in the region (ii) (where the curves are dense) also exist in all the other regions. While the dynamics associated with the case under assumptions $F(ii)$ are already known in the literature, we don't know a similar result for all the other cases $F(id)$,$F(di)$ and $F(dd)$. However, given that the curves associated with periodic orbits are dense in the region (ii), also the curves obtained by symmetry are dense in the other regions (id), (di) and (dd). Moreover, we can analytically write the curves at which we can find all periodic orbits and of any level of complexity, and the periods of the cycles associated to these curves are those commented above. This proves the following result:

Proposition 5. *Consider the map F with $|a| > 1$ and $|b| < 1$, then all the trajectories enter an invariant absorbing set A inside which we can have either all periodic orbits or all quasiperiodic trajectories. By using the adding scheme we can write all the analytic curves in the parameter plane (a,b) associated with the periodic orbits of any level of complexity. For suitable integers p and q, all the curves can be written as $a^p b^q = 1$.*

6. Generalization and regularity breaking

In this section we generalize the map given in (3). Let us consider the following map:

$$M: \quad X' = \begin{cases} F(X) & \text{if } |X| < \tau, \\ G(X) & \text{if } |X| > \tau, \end{cases} \tag{36}$$

where $F(X)$ and $G(X)$ are monotonic functions, either increasing or decreasing, such that $F(0) = G(0) = 0$. The parameter τ satisfies $\tau > 0$. As it is a scale parameter, by using the change of variable $x = X/\tau$, our model in (36) becomes the following map T:

$$T: \quad x' = \begin{cases} f(x) & \text{if } |x| < 1, \\ g(x) & \text{if } |x| > 1, \end{cases} \tag{37}$$

where $f(x) = F(\tau x)$ and $g(x) = G(\tau x)$. Then the following proposition holds:

Proposition 6. *Consider the map T in (37) with increasing f and g monotone (increasing or decreasing) such that $f(0) = g(0) = 0$. If the following equalities hold:*

$$(S): \ f \circ g(1) = g \circ f(1), \quad f \circ g(-1) = g \circ f(-1) \tag{38}$$

then the system can be reduced to a circle map in a suitable interval.

Proof. To prove the statement, we separately consider the cases (ii), (id) for the monotone functions f and g respectively, where i/d denotes increasing/decreasing.

– (*ii*). This is the simplest case, as when the two functions are both increasing, then two disjoint invariant absorbing intervals exist, $I^R = [g(1), f(1)]$ and $I^L = [f(-1), g(-1)]$, and the conditions in (*S*) correspond to the definition of *T* a circle map in each invariant interval.
– (*id*). In this case there exists an invariant absorbing set

$$A = [f(-1), g(1)] \cup [g(-1), f(1)]. \tag{39}$$

In the interval $[f(-1), g(1)] = [f(-1), f(g(1))] \cup [g(f(1)), g(1)]$ (where we have used $f(g(1)) = g(f(1))$), each point of $[f(-1), f(g(1))]$ has only the inverse via f^{-1} in *A*, while each point of $[g(f(1)), g(1)]$ has only the inverse via g^{-1} in *A*. Similarly in the other interval $[g(-1), f(1)] = [g(-1), g(f(-1)] \cup [f(g(-1)), f(1)]$ (where we have used $g(f(-1)) = f(g(-1))$), each point of $[g(-1), g(f(-1)]$ has only the inverse via g^{-1} in *A* while each point of $[f(g(-1)), f(1)]$ has only the inverse via f^{-1} in *A*. So the properties of map *T* can be studied by using the first return, say map T_r, in a suitable interval. As a trajectory from the side $x < 0$ can return on the side $x > 0$ only via application of *g*, we can consider the first interval on the right side, that is:

$$r = [g(-1), g(f(-1))]. \tag{40}$$

We shall prove that T_r is defined by piecewise increasing functions having a unique discontinuity point in the first preimage of $x = -1$ belonging to *r*, but continuous in the preimage of $x = 1$, and that T_r is a circle map. Let ηbe the first preimage of $x = 1$ belonging to *r*. That is, an integer $m \geqslant 0$ ($m = 0$ corresponds to the case $1 \in r$) exists such that

$$\eta = f^{-m}(1) \tag{41}$$

and let us define as $\xi$the first preimage of the point $x = -1$ in *r*, which may be smaller or larger than η. That is, for a suitable $n \geqslant 0$, we have either

$$(j)\ \xi = f^{-(m+1)} \circ g^{-1} \circ f^{-n}(-1) < \eta \tag{42}$$

or

$$(jj)\ \xi = f^{-m} \circ g^{-1} \circ f^{-n}(-1) > \eta \tag{43}$$

In the case (*j*) the first return map is defined as

$$T_r: \quad x' = \begin{cases} H_l(x) = g \circ f^{(n+1)} \circ g \circ f^{(m+1)}(x) & \text{if } g(-1) \leqslant x < \xi \\ H_r(x) = g \circ f^n \circ g \circ f^{(m+1)}(x) & \text{if } \xi < x \leqslant \eta \\ H_{rr}(x) = g \circ f^{(n+1)} \circ g \circ f^m(x) & \text{if } \eta \leqslant x \leqslant g(f(-1)) \end{cases} \tag{44}$$

and it is immediate to verify that $H_l(\xi) = g(f(-1))$, $H_r(\xi) = g(-1)$, $H_r(\eta) = g \circ f^n \circ g \circ f(1)$, $H_{rr}(\eta) = g \circ f^{(n+1)} \circ g(1) = g \circ f^n(f(g(1)))$ so that, due to the property (*S*) we have $g \circ f(1) = f \circ g(1)$ and thus $H_r(\eta) = H_{rr}(\eta)$ (continuity of T_r in η), $H_{rr} \circ H_l(\xi) = g \circ f^{(n+1)} \circ g \circ f^m(g(f(-1)))$, $H_l \circ H_r(\xi) = g \circ f^{(n+1)} \circ g \circ f^{(m+1)}(g(-1)) = g \circ f^{(n+1)} \circ g \circ f^m(f(g(-1))) = H_{rr} \circ H_l(\xi)$ due to the property (*S*), so that T_r is a circle map in *r*.

In the case (*jj*) the first return map is defined as

$$T_r: \quad x' = \begin{cases} H_{ll}(x) = g \circ f^n \circ g \circ f^{(m+1)}(x) & \text{if } g(-1) \leqslant x \leqslant \eta \\ H_l(x) = g \circ f^{(n+1)} \circ g \circ f^m(x) & \text{if } \eta \leqslant x < \xi \\ H_r(x) = g \circ f^n \circ g \circ f^m(x) & \text{if } \xi < x \leqslant g(f(-1)) \end{cases}$$

and it is immediate to verify that $H_l(\xi) = g(f(-1))$, $H_r(\xi) = g(-1)$, $H_l(\eta) = H_{ll}(\eta)$ (continuity of T_r in η), $H_r \circ H_l(\xi) = g \circ f^n \circ g \circ f^{(n+1)}(g(f(-1)))$, $H_{ll} \circ H_r(\xi) = g \circ f^n \circ g \circ f^m(f(g(-1))) = H_r \circ H_l(\xi)$ due to the property (*S*), so that T_r is a circle map in *r*. □

It is worth to note that similar properties exist also the function *f* is decreasing (and *g* increasing or decreasing), that is, in the cases (*di*) and (*dd*). However, the proof in general is more difficult. When only two preimages of the discontinuity points exist in the absorbing interval, then the second iterate of the map is also a map with only two discontinuities. These cases are reduced to the two previous ones by use of the second iterate T^2 of map *T*. In fact, considering the rank-1 preimages of the discontinuity points $x = 1$ and $x = -1$ of the function *f* existing inside the range $|x| < 1$, say

$$-1 < x_l = f^{-1}(1) < 0, \quad 0 < x_r = f^{-1}(-1) < 1 \tag{45}$$

then the second iterate is defined as follows:

$$T^2: \quad x' = \begin{cases} f \circ g(x) & \text{if } g(-1) \leqslant x \leqslant -1 \\ g \circ f(x) & \text{if } -1 \leqslant x < x_l \\ f^2(x) & \text{if } x_l < x < x_r \\ g \circ f(x) & \text{if } x_r < x \leqslant 1 \\ f \circ g(x) & \text{if } 1 \leqslant x \leqslant g(f(-1)) \end{cases} \tag{46}$$

where x_l and x_r are the only two discontinuity points of the map T^2, as the conditions in (*S*) lead to continuity of T^2 in $x = 1$ and $x = -1$. Thus:

– In the case (*di*), outside the interval (x_l, x_r) the second iterate T^2 is a decreasing function, so that T^2 is a map of type increasing/decreasing as already considered in the case (*id*), with discontinuity points in x_l and x_r in place of -1 and 1, respectively;
– In the case (*dd*), outside the interval (x_l, x_r) the second iterate T^2 is an increasing function, so that T^2 is a map of type increasing/increasing as already considered in the case (*ii*), with discontinuity points in x_l and x_r in place of -1 and 1, respectively.

In any case, when condition (*S*) holds, an invariant absorbing set *A* can be defined inside which the map is uniquely invertible, and without gap, so that no chaotic behavior can occur. In the particular case of linear functions for *f* and *g* we get a linear circle map, and the same results described in the previous sections. While when *f* and *g* are generic monotone functions the trajectories are of the same kind of those existing in a circle map (see [20,9,13]). So we still have that all the points in *A* have the asymptotic behavior depending on the rotation number, which is uniquely defined, either rational or irrational. However, in a generic circle map only the irrational case is structurally unstable. When a rational rotation number exists it is generally persistent as a function of the parameters in some set. Also the attracting sets are different. When a rational rotation number exists then all the trajectories have a cycle as ω-limit set (not necessarily unique, but all of the same period). When the rotation number is irrational and the functions *f* and *g* are of class $\mathcal{C}^2$ then quasi periodic trajectories are dense in the whole set *A*, while if the functions *f* and *g* have not log (f') and log (g') with bounded variation, then the

quasiperiodic trajectories may be dense in a Cantor set attractor (or in the invariant set A).

In the family of piecewise monotone functions of the interval known as Lorenz maps, the occurrence of a circle map is a kind of bifurcation case, and separates two classes of functions: those which are invertible with a gap, and those which are noninvertible (or overlapping), and the three classes have different dynamic properties. When a Lorenz map is invertible with a gap, then the attractor is a unique cycle (when the rotation number is rational) or a Cantor set attractor (when the rotation number is irrational), and the rational rotation is persistent, or structurally stable, while the irrational rotation is structurally unstable. When a Lorenz map is noninvertible, then a chaotic repeller exists although the attracting set may be a cycle or chaotic intervals (in both cases structurally stable), or a Cantor set attractor (structurally unstable).

Similarly in our case, with generic smooth functions, it can be considered that the occurrence of the conditions in (38) corresponds to a bifurcation case, such that before and after that condition the map behaves differently. That is, when the conditions are not satisfied we can have dynamics associated with invertible maps with a gap or associated with a noninvertible map. Let us illustrate here two examples, one of which includes the linear case of the previous sections as a particular bifurcation, and a second one in which the bifurcation associated with the stability conditions (S) behaves differently.

6.1. First example

Let us consider the family of maps

$$T: \quad x' = \begin{cases} f(x) = a|x|^{a_1}\,\mathrm{sgn}(x) & \text{if } |x| < 1 \\ g(x) = b|x|^{b_1}\,\mathrm{sgn}(x) & \text{if } |x| > 1 \end{cases} \tag{47}$$

as a function of four parameters, for which it is clear that when $a_1 = 1$ and $b_1 = 1$ we get the map F in (3) so that the dynamic behavior of the map in this bifurcation case (with the stability conditions (S) satisfied) is completely known. We can expect that the dynamic behaviors are different when the parameters a_1 and b_1 are not both equal to 1. In Fig. 11 we show the shape of map T at $a = 2$ and $b = 0.23$ fixed (so that we are in a case (ii)) and $a_1 = b_1 = 0.9$ in Fig. 11a, where we can see that the function is invariant in two disjoint intervals $I^R = [g(1), f(1)]$ and $I^L = [f(-1), g(-1)]$, in which it is *a Lorenz map with a gap* ($f \circ g(1) > g \circ f(1)$ and $g \circ f(-1) > f \circ g(-1)$) and the attractor is a 3-cycle in both intervals, while $a_1 = b_1 = 1.1$ in Fig. 11b, where we can see that the function is invariant in these two disjoint intervals in which it is *a noninvertible Lorenz map* ($f \circ g(1) < g \circ f(1)$ and $g \circ f(-1) < f \circ g(-1)$), with chaotic dynamics in both intervals. Also with $a_1 = 0.9$ and $b_1 = 1.1$we obtain that the function is invariant in I^R and I^L in which it is a Lorenz map with a gap (the attractors are different cycles in the two intervals), while for $a_1 = 1.1$ and $b_1 = 0.9$ we obtain the function invariant in I^R and I^L in which it is a noninvertible Lorenz map, with chaotic dynamics in both intervals.

As an example of the bifurcation structure, in Fig. 12 we illustrate the two-dimensional parameter plane (a, b) at $a_1 = b_1 = 0.9$ fixed. The regions with $|a| > 1$ and $|b| < 1$are filled with periodicity regions associated with attracting cycles of any period. That is, the dynamic behavior of a Lorenz map with a gap persists not only in the (ii) case with $a > 1$ and $0 < b < 1$, but in all the other regions as well. The point $A = (2, 0.23)$ (used to plot the map in Fig. 11a) is shown in the enlargement in Fig. 12b, and it is inside a periodicity region of a 3-cycle. It is worth to note that also in this nonlinear case we can analytically determine the border collision bifurcation curves bounding the periodicity regions of the existing cycles. Let us consider the region (ii) and proceed in the same way as described in Section 3. In order to have a periodic point of a so-called maximal cycle in the interval I^R, say with symbolic sequence fg^k, $k \geqslant 1$, we have to look for a fixed point of the composite function $g^k \circ f(x)$, by solving the equation $g^k \circ f(x) = x$. It is well known (see [15]) that the appearance/disappearance of the cycle occurs via BCB when a periodic point of the cycle collides with the discontinuity point $x = 1$. Thus the equations of the two BCB curves bounding a maximal cycle fg^k are given by

$$g^k \circ f(1) = 1 \tag{48}$$

$$g^{k-1} \circ f \circ g(1) = 1 \tag{49}$$

By using the explicit formulation

$$g^k(x) = b^{(1+b_1+\cdots+b_1^{k-1})} x^{b_1^k} = b^{\frac{1-b_1^k}{1-b_1}} x^{b_1^k} \tag{50}$$

we have the equations

$$b^{\frac{1-b_1^k}{1-b_1}} a^{b_1^k} = 1 \tag{51}$$

$$b^{\frac{1-b_1^{k-1}}{1-b_1}} (ab^{a_1})^{b_1^{k-1}} = 1 \tag{52}$$

In Fig. 13 the curves in (51) and (52) are reported for $k = 1, \ldots, 10$ in the upper part of the figure, bounding periodicity regions of cycles of period $2, \ldots, 11$ of symbolic sequence fg^k. Similarly we can reason for the cycles in the same interval with symbolic sequence gf^k, for any $k \geqslant 1$, the BCB curves satisfy

$$f^k \circ g(1) = 1 \tag{53}$$

$$f^{k-1} \circ g \circ f(1) = 1 \tag{54}$$

and by using the explicit formulation

$$f^k(x) = a^{(1+a_1+\cdots+a_1^{k-1})} x^{a_1^k} = a^{\frac{1-a_1^k}{1-a_1}} x^{a_1^k} \tag{55}$$

we have the equations

$$a^{\frac{1-a_1^k}{1-a_1}} x^{a_1^k} = 1 \tag{56}$$

$$a^{\frac{1-a_1^{k-1}}{1-a_1}} (ba^{b_1})^{a_1^{k-1}} = 1 \tag{57}$$

In Fig. 13 the curves in (56) and (57) are reported for $k = 1, \ldots, 10$ in the lower part of the figure, bounding periodicity regions of cycles of period $2, \ldots, 11$ of symbolic sequence gf^k (clearly for $k = 1$ the two families give the same BCB curves). It is obvious that as a_1 and b_1 tend to 1 the two BCB curves bounding the periodicity regions become closer

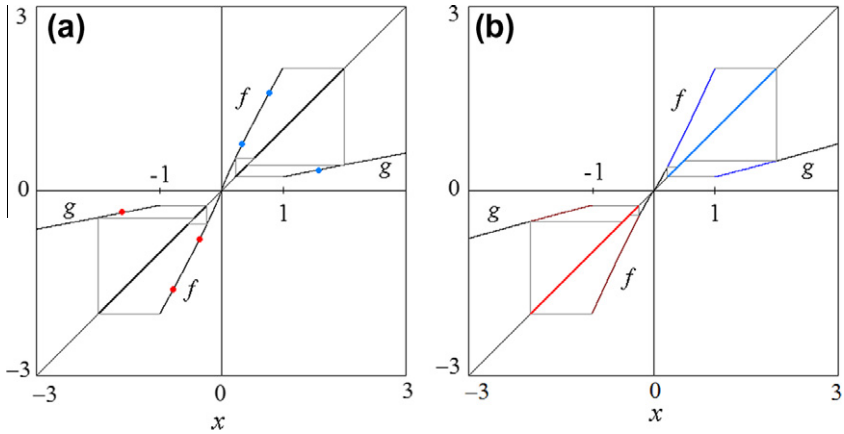

Fig. 11. Map T in (47) at $a = 2$ and $b = 0.23$. In (a) $a_1 = b_1 = 0.9$. In (b) $a_1 = b_1 = 1.1$.

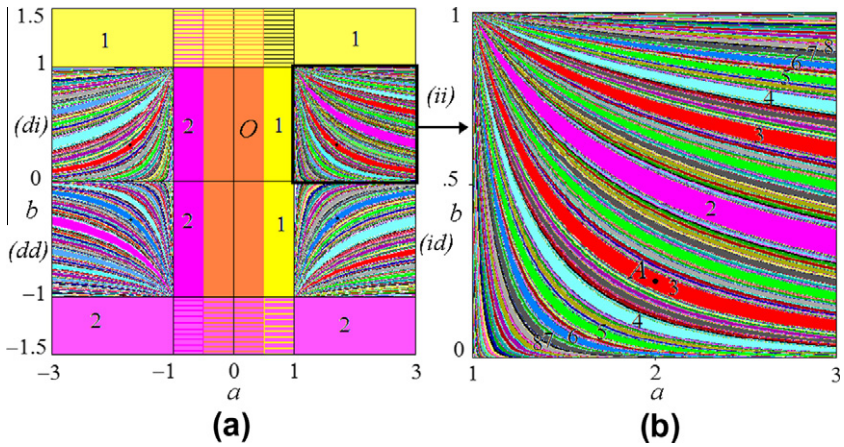

Fig. 12. Two-dimensional bifurcation diagram of map T in (47) in the (a,b) parameter plane at $a_1 = b_1 = 0.9$ fixed. i.c. $x_0 = -0.9$.

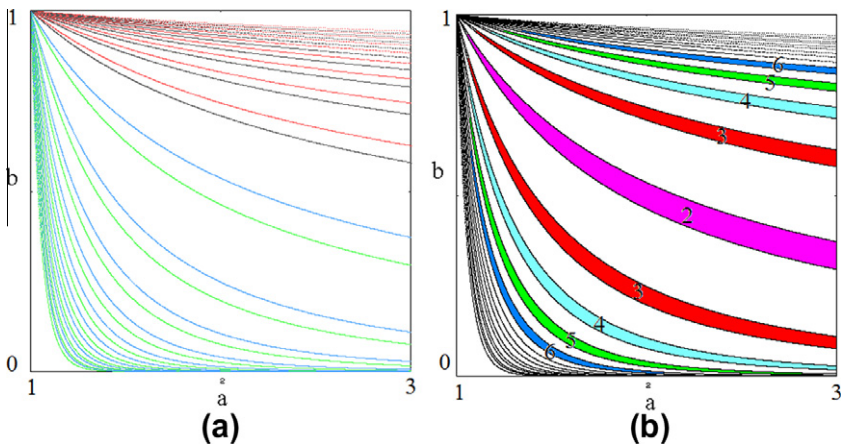

Fig. 13. Bifurcation curves in (51) and (52) in the upper part and in (56) and (57) in the lower part, for $k = 1,\ldots,10$.

and closer and for $a_1 = b_1 = 1$ these coincide in the unique curve whose equation has been given in Section 3.

By using the map-replacement technique (see [15,4]) it is also possible to analytically detect the BCB curves of any

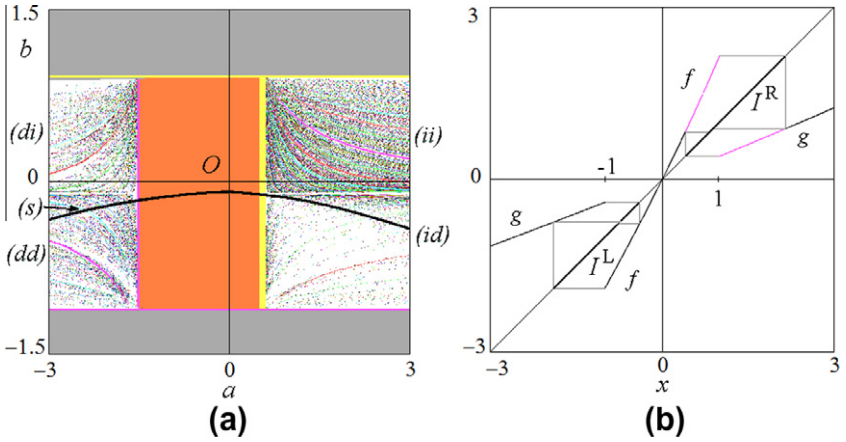

Fig. 14. In (a) two-dimensional bifurcation diagram of map T in (58) in the (a,b) parameter plane at $a_1 = 0.5$, $b_1 = 0.1$ fixed, and i.c. $x_0 = -0.9$. In (b) shape of the map for $a_1 = 0.5$, $b_1 = 0.1$, $a = 1.5$, $b = 0.3$.

complexity level, which are dense in the region and have as limit sets curves associated with irrational rotation numbers (and structurally unstable dynamics).

In Fig. 12 we can see that besides the periodicity regions of cycles following the adding mechanism (or Farey tree structure), the regions are colored in orange (representing the attracting fixed point in the origin) or in yellow (representing an attracting fixed point not in the origin) or in pink (representing an attracting 2-cycle), which also may coexist. However, what is interesting to remark here, is the dynamic behavior in the other regions different from (*ii*) when no fixed points nor 2-cycles exist. The bifurcation structure of the cycles existing in the disjoint intervals I^R and I^L in case (*ii*) is well known (and what is new here is the explicit analytic equations of the BCB curves, which can be done for any complexity level), but the interesting point is that a similar structure also occurs in the other regions, but associated with different periods. As we have seen, in the point $A = (2, 0.23) \in region(ii)$ we have a 3-cycle of symbolic sequence gf^2, then in the point $(2, -0.23) \in region(id)$ the map, with two discontinuity points, is now invertible in an invariant set A, with a gap, and we have a cycle of double period (as expected as the number of points under the function g, now decreasing, was odd). As we have done in Section 4, probably this case may be studied via the first return map in the interval $r = [g(-1), g(f(-1))]$. In the point $(-2, 0.23) \in region(di)$ we have a cycle of the same period 3, while in the point $(-2, -0.23) \in region(dd)$ we have a cycle of double period 6. However, we notice that now the map is invariant in an attracting set A in which it is invertible with a gap, and we have two discontinuities. Thus the related properties are still to be investigated.

6.2. Second example

As a second example let us consider the system defined by

$$T: \quad x' = \begin{cases} f(x) = ax + e^{a_1 x} - 1 & \text{if } |x| < 1 \\ g(x) = bx + e^{b_1 x} - 1 & \text{if } |x| > 1 \end{cases} \tag{58}$$

Assuming the parameters $a_1 = 0.5$ and $b_1 = 0.1$ fixed, we have numerically computed the set of parameters (a,b) at which the stability condition (S) in (38) is satisfied, and it is reported in Fig. 14a (black curve evidenced by an arrow). As we can see, it occurs only when the functions f and g are in the regions (id) and (dd). When the parameters belong to such a curve the map behaves as a circle map, and now we may have persistence of an attracting cycle. More complicated is the investigation of the dynamics when the parameters are outside the stability curve. We notice that both above and below the curve we can have, for the map T, an invariant absorbing set $A = [f(-1), g(1)] \cup [g(-1), f(1)]$ including both an interval without preimages in A and an interval with two preimages in A (located on opposite sides with respect to the origin). However, in the region (id), as long as an invariant absorbing set A exists, the properties of the map can be investigated making use of the first return map T_r in the interval $r = [g(-1), g(f(-1))]$.

Differently, when the parameters belong to the region (*ii*) visible in Fig. 14a, we have now that the map is invariant in two disjoint intervals $I^R = [g(1), f(1)]$ (where it is a noninvertible Lorenz map, thus with the existence of chaotic dynamics) and $I^L = [f(-1), g(-1)]$ in which it is an invertible Lorenz map, an example is shown in Fig. 14b. The colored regions in (*ii*) visible in Fig. 14a correspond to attracting cycles in the interval I^L.

7. Conclusions

In this work we have shown the dynamics of a particular family of maps, defined in (3). In its simplicity, which makes the model suitable for several applications, we have shown that when the parameters a and b satisfy $|a| > 1$ and $|b| < 1$ then the stability conditions (S1) and (S2) (in (9) and (10)) are always satisfied, which implies that only regular dynamics can exist. In the case $a > 0$ and $b > 0$ (i.e., $f(x)$ and $g(x)$ both increasing functions) this was a known result, but we have proved that the dynamics are similar also when the slopes have all the other different signs. Moreover, we have proved that the curves in the (a,b) parameter plane, associated with periodic orbits, can be easily found analytically, and for any level of complexity. However, the regular dynamics so determined are structurally unstable. Assuming generic monotone functions as defined in

(37) we have proved that the stability condition leads to circle maps, and now the existence of attracting cycles (at rational rotation numbers) may be persistent. In general, the stability condition can be seen as a bifurcation case. When the functions are both increasing the stability breaking leads the dynamics to those of Lorenz maps, invertible and noninvertible, while in the other cases the breaking of the condition leads to new phenomena, and it is left for further studies.

References

[1] Avrutin V, Schanz M. Multi-parametric bifurcations in a scalar piecewise-linear map. Nonlinearity 2006;19:531–52.
[2] Avrutin V, Schanz M. On the fully developed bandcount adding scenario. Nonlinearity 2008;21:1077–103.
[3] Avrutin V, Schanz M, Banerjee S. Multi-parametric bifurcations in a piecewise-linear discontinuous map. Nonlinearity 2006;19:1875–1906.
[4] Avrutin V, Schanz M, Gardini L. Calculation of bifurcation curves by map replacement. Int J Bifurcat Chaos 2010;20:3105–35.
[5] Alsedà LL, Llibre J, Misiurewicz M, Tresser C. Periods and entropy for Lorenz-like maps. Ann Inst Fourier 1989;39(4):929–52.
[6] Banerjee S, Yorke JA, Grebogi C. Robust Chaos. Phys Rev Lett 1998;80:3049–52.
[7] Banerjee S, Karthik MS, Yuan G, Yorke JA. Bifurcations in One-Dimensional Piecewise Smooth Maps - Theory and Applications in Switching Circuits. IEEE Trans Circ Syst I 2000;47:389–94.
[8] Banerjee S, Verghese GC, editors. Nonlinear phenomena in power electronics: attractors. Bifurcations, Chaos, and Nonlinear Control. New York: IEEE Press; 2001.
[9] Berry D, Mestel BD. Wandering interval for Lorenz maps with bounded nonlinearity. Bull London Math Soc 1991;23:183–9.
[10] Cvitanović P, Shraiman B, Söderberg B. Scaling laws for mode lockings in circle maps. Phys Scripta 1985;32:263–70.
[11] Day R. Irregular growth cycles. Am Econ Rev 1982;72:406–14.
[12] Day R. Complex Economic Dynamics. Cambridge: MIT Press; 1994.
[13] de Melo W, van Strien S. One-Dimensional Dynamics. New York: Springer-Verlag; 1991.
[14] di Bernardo M, Budd CJ, Champneys AR, Kowalczyk P. Piecewise-smooth dynamical systems: theory and applications. Appl Math Sci, vol. 163. London: Springer-Verlag; 2007.
[15] Gardini L, Tramontana F, Avrutin V, Schanz M. Border collision bifurcations in 1D PWL map and Leonov's approach. Int J Bifurcat Chaos 2010;20:3085–104.
[16] Gardini L, Tramontana F. Border Collision Bifurcations in 1D PWL map with one discontinuity and negative jump. Use of the first return map. Int J Bifurcat Chaos 2010;20:3529–47.
[17] Glendinning P, Sparrow C. Prime and renormalisable kneading invariants and the dynamics of expanding Lorenz maps. Physica D 1993;62:22–50.
[18] Ito S, Tanaka S, Nakada H. On unimodal transformations and chaos II. Tokyo J Math 1979;2:241–59.
[19] Yiming D, Wentao F. The asymptotic periodicity of Lorenz maps. Acta Math. Sci 1999;19(1):114–20.
[20] Keener JP. Chaotic behavior in piecewise continuous di erence equations. Trans Am Math Soc 1980;261:589–604.
[21] Kim S, Ostlund S. Universal scaling in circle maps. Physica D 1989;39:365–92.
[22] Leonov NN. Map of the line onto itself. Radiofisica 1959;3:942–56.
[23] Leonov NN. Discontinuous map of the straight line. Dolk Acad Nauk SSSR 1962;143:1038–41.
[24] Mackay RS, Tresser C. Transition to topological chaos for circle maps. Physica 1986;19D:206–37.
[25] Maistrenko YL, Maistrenko VL, Chua LO. Cycles of chaotic intervals in a time-delayed Chua's circuit. Int J Bifurcat Chaos 1993;3:1557–72.
[26] Maistrenko YL, Maistrenko VL, Vikul SI, Chua LO. Bifurcations of attracting cycles from time-delayed Chua's circuit. Int J Bifurcat Chaos 1995;5:653–71.
[27] Maistrenko YL, Maistrenko VL, Vikul SI. On period-adding sequences of attracting cycles in piecewise linear maps. Chaos Soliton Fract 1998;9:67–75.
[28] Mira C. Sur les structure des bifurcations des diffeomorphisme du cercle. C R Acad Sci Paris Ser A 1978;287:883–6.
[29] Mira C. Chaotic dynamics. Singapore: World Scientific; 1987.
[30] Nordmark AB. Non-periodic motion caused by grazing incidence in an impact oscillator. J Sound Vib 1991;145:279–97.
[31] Nusse HE, Yorke JA. Border-collision bifurcations including period two to period three for piecewise smooth systems. Physica D 1992;57:39–57.
[32] Nusse HE, Yorke JA. Border-collision bifurcation for piecewise smooth one-dimensional maps. Int. J Bifurcat Chaos 1995;5:189–207.
[33] Procaccia I, Thomae S, Tresser C. First-return map as a unified renormalization scheme for dynamicalsystems. Phys Rev A 1987;34(4):1884–900.
[34] Puu T, Sushko I. Oligopoly Dyn. Models and tools. New York: Springer Verlag; 2002.
[35] Puu T, Sushko I. Business cycle dynamics. Models and Tools. New York: Springer Verlag; 2006.
[36] Sushko I, Gardini L. Degenerate bifurcations and border collisions in piecewise smooth 1D and 2D maps. Int J Bifurcat Chaos 2010;20:2045–2070.
[37] Takens F. Transitions from periodic to strange attractors in constrained equations. In: Camacho MI, Pacifico MJ, Takens F, editors. Dynamical systems and bifurcation theory. Research notes in mathematis series, vol. 160. Pitman: Longman Scientific and Techical; 1987. p. 399–421.
[38] Tramontana F, Gardini L, Ferri P. The dynamics of the NAIRU model with two switching regimes. J Econ Dyn Contr 2010;34:681–95.
[39] Tramontana F, Westerhoff F, Gardini L. On the complicated price dynamics of a simple one-dimensional discontinuous financial market model with heterogeneous interacting traders. J Econ Behav Organ 2010;74:187–205.
[40] Tramontana F. Westerhoff F. Gardini L. A simple financial market model with chartists and fundamentalists: market entry levels and discontinuities, Working Paper University of Pavia, 2012.
[41] Tramontana F, Gardini L, Avrutin V, Schanz M. Period adding in piecewise linear maps with two discontinuities. Int J Bifurcat Chaos 2012;22(3):1250068. 30 pages.
[42] Zhusubaliyev ZT, Mosekilde E. Bifurcations and chaos in piecewise-smooth dynamical systems. Singapore: World Scientific; 2003.